

On the Value of Cooperation in Interference Relay Networks*

Veniamin I. Morgenshtern and Helmut Bölcskei

Communication Technology Laboratory
Swiss Federal Institute of Technology (ETH) Zurich
Sternwartstrasse 7, 8092 Zürich, Switzerland
Email: {vmorgens | boelcskei}@nari.ee.ethz.ch

Abstract

We study fading interference relay networks where M single-antenna source-destination terminal pairs communicate concurrently through a set of K relays, each of which is equipped with N (cooperating) transmit/receive antennas, using half-duplex two-hop relaying under the two protocols introduced in [1] and [2], respectively. The main contributions of this paper are:

- For fixed N and $M, K \rightarrow \infty$, we establish the impact of cooperation at the relay level on network capacity scaling. More specifically, it is shown that asymptotically in M and K cooperation in groups of N relay antenna elements leads to an N -fold reduction in the total number of relays needed to achieve a given per source-destination terminal pair capacity.
- We characterize the rate at which the network “crystallizes”, i.e., the individual single-input single-output source-destination terminal pair links decouple and the corresponding random (fading) channel gains converge to a deterministic limit.

1 Introduction

Capacity scaling in large wireless (relay) networks and code design for cooperative communication has recently attracted significant attention [1–13]. In this paper, we consider fading interference relay networks, where M single-antenna source-destination terminal pairs communicate concurrently through half-duplex two-hop relaying over a set of K relay terminals each of which is equipped with N (cooperating) transmit/receive antennas. Two specific protocols, P1 [1] and P2 [2], have been introduced for this setup for the $N = 1$ case. The corresponding per source-destination terminal pair capacity was shown to scale (for $M, K \rightarrow \infty$) as¹ [13]

$$C_{\text{P1}} = \frac{1}{2} \log \left(1 + \Theta \left(\frac{K}{M^3} \right) \right), \quad C_{\text{P2}} = \frac{1}{2} \log \left(1 + \Theta \left(\frac{K}{M^2} \right) \right)$$

*This research was supported by Nokia Research Center Helsinki, Finland.

¹The notation $\Theta(\cdot)$ is defined in the notations paragraph in this section.

for P1 and P2, respectively. The purpose of this paper is twofold, (i) to study the impact of cooperation at the relay level on the per source-destination terminal pair capacity scaling law, and (ii) to perform an outage analysis by characterizing the behavior of the signal to interference plus noise ratio (SINR) of the individual (fading) source-destination terminal pair links when $M, K \rightarrow \infty$ and N is fixed. Our specific contributions can be summarized as follows:

- We first formulate (straightforward) modifications of P1 and P2 to take into account the presence of multiple (cooperating) antennas at the relays². Based on techniques developed in [2, 13, 14], we then establish lower and upper bounds on the per source-destination terminal pair capacity for N fixed and $M, K \rightarrow \infty$. These bounds are tight up to a constant, which depends on the geometry of the network only, and make the impact of cooperation at the relay level explicit. In particular, it is shown that (asymptotically in M and K) cooperation in groups of N relay antenna elements leads to an N -fold reduction in the total number of relays needed to achieve a given per source-destination terminal pair capacity. We also state a stronger lower bound on the per source-destination terminal pair capacity of P1 and P2, which is valid in the finite M, K case.
- The second contribution of this paper has the flavor of an outage analysis. More specifically, we analyze the convergence behavior (when $M, K \rightarrow \infty$ and N is fixed) of the individual (random) source-destination terminal pair link SINRs. This result establishes the rate at which the network “crystallizes”, i.e., the individual source-destination terminal pair links decouple (in a sense to be made precise in Sections 4 and 5) and the corresponding random SINR values approach deterministic quantities.

Notation. The superscripts T , H and $*$ stand for transposition, conjugate transpose, and element-wise conjugation, respectively. $|\mathcal{X}|$ is the cardinality of the set \mathcal{X} . All logarithms are to the base 2. \mathcal{E} and VAR denote the expectation and variance operator, respectively. $\arg(x)$ stands for the argument of $x \in \mathbb{C}$. A circularly symmetric zero-mean complex Gaussian random variable (RV) is a RV $Z = X + jY \sim \mathcal{CN}(0, \sigma^2)$, where X and Y are i.i.d. $\mathcal{N}(0, \sigma^2/2)$. $\delta[k] = 1$ for $k = 0$ and 0 otherwise. For two functions $f(x)$ and $g(x)$, the notation $f(x) = O(g(x))$ means that $|f(x)/g(x)|$ remains bounded as $x \rightarrow \infty$. We write $g(x) = \Theta(f(x))$ to denote that $f(x) = O(g(x))$ and $g(x) = O(f(x))$.

Organization of the paper. The remainder of this paper is organized as follows. Section 2 introduces the general channel and signal model. In Section 3, we describe the (straightforward) extension of protocols P1 and P2, as described in [13], to the multiple-antenna relay case. In Section 4, we state our ergodic capacity scaling results for the two protocols. Our findings on the outage behavior of P1 and P2 are provided in Section 5. Numerical results are given in Section 6. We conclude in Section 7.

2 Channel and Signal Model

In this section, we present the channel and signal model and additional basic assumptions. The discussion is general and applies to both protocols under consideration. The specifics of P1 and P2 are described in Section 3.

²The original proposal of P1 in [1] (for the finite M case) already takes the presence of multiple (cooperating) antennas at the relays into account.

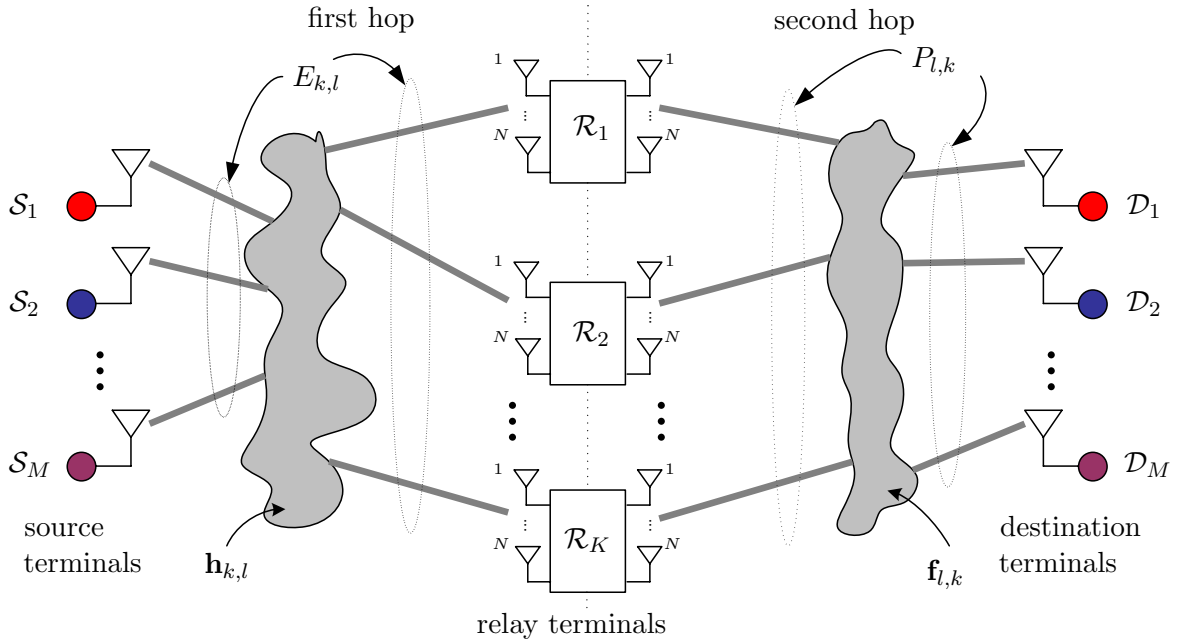


Figure 1: Interference relay network with cooperation at the relay level.

2.1 General assumptions

We consider an interference relay network (see Fig. 1) consisting of M designated source-destination terminal pairs $\{\mathcal{S}_l, \mathcal{D}_l\}$ ($l = 1, 2, \dots, M$) and K relays \mathcal{R}_k ($k = 1, 2, \dots, K$), each of which is equipped with N cooperating transmit/receive antennas. Source terminal \mathcal{S}_l intends to communicate solely with destination terminal \mathcal{D}_l , a dead-zone of non-zero radius around each \mathcal{S}_l and \mathcal{D}_l is free of relay terminals, and no cooperation between terminals (not even between the destination terminals) is allowed. The individual antenna elements on a given relay terminal are, however, allowed to cooperate. Furthermore, we assume that no direct link between the source terminals and the destination terminals exists (e.g., caused by large separation), transmission takes place in half-duplex fashion (the terminals cannot transmit and receive simultaneously) in two hops (two-hop relaying) over two separate time slots. In the first time slot the source terminals \mathcal{S}_l broadcast their information to all the relay terminals (i.e., each relay terminal receives a superposition of all source signals). After processing the received signals, the relay terminals simultaneously broadcast the processed data to all the destination terminals during the second time slot. Finally, we assume that all terminals are located within a domain of fixed area (dense network assumption).

2.2 Channel and signal model

Throughout the paper, we assume ergodic frequency-flat fading and perfectly synchronized transmission/reception between the terminals. The input-output relation for the³ $\mathcal{S}_l \rightarrow \mathcal{R}_k$ link during the first time slot is given by

$$\mathbf{r}_k = \sum_{l=1}^M \sqrt{E_{k,l}} \mathbf{h}_{k,l} s_l + \mathbf{n}_k, \quad k = 1, 2, \dots, K \quad (1)$$

³ $\mathcal{A} \rightarrow \mathcal{B}$ signifies communication from terminal \mathcal{A} to terminal \mathcal{B} .

where the $N \times 1$ vector \mathbf{r}_k denotes the received signal at the k th relay terminal, $E_{k,l}$ is the average energy received at \mathcal{R}_k through the $\mathcal{S}_l \rightarrow \mathcal{R}_k$ link (having accounted for path loss and shadowing in the $\mathcal{S}_l \rightarrow \mathcal{R}_k$ link), $\mathbf{h}_{k,l}$ denotes the corresponding $N \times 1$ complex-valued channel vector, independent across source and relay terminals (i.e., independent across $l = 1, 2, \dots, M$ and $k = 1, 2, \dots, K$) with i.i.d. $\mathcal{CN}(0, 1)$ components, s_l is the temporally i.i.d. $\mathcal{CN}(0, 1)$ data signal transmitted by \mathcal{S}_l and satisfying $\mathcal{E}\{s_l s_k^*\} = \delta[l - k]$, and \mathbf{n}_k is the $N \times 1$ temporally and spatially (across relay terminals) white noise vector with i.i.d. $\mathcal{CN}(0, \sigma^2)$ elements.

Each relay terminal processes its received signal \mathbf{r}_k to produce the output signal \mathbf{t}_k , which is then broadcast to the destination terminals during the second time slot while the source terminals are silent. The l th destination terminal receives the signal

$$y_l = \sum_{k=1}^K \sqrt{P_{l,k}} \mathbf{f}_{l,k}^T \mathbf{t}_k + z_l, \quad l = 1, 2, \dots, M \quad (2)$$

where $P_{l,k}$ denotes the average energy received at \mathcal{D}_l through the $\mathcal{R}_k \rightarrow \mathcal{D}_l$ link (having accounted for path loss and shadowing in the $\mathcal{R}_k \rightarrow \mathcal{D}_l$ link), $\mathbf{f}_{l,k}^T$ is the corresponding $1 \times N$ complex-valued channel vector, independent across destination and relay terminals (i.e., independent across $l = 1, 2, \dots, M$ and $k = 1, 2, \dots, K$) with i.i.d. $\mathcal{CN}(0, 1)$ components, and z_l is $\mathcal{CN}(0, \sigma^2)$ temporally and spatially (across destination terminals) white noise. The transmit signal \mathbf{t}_k is chosen to satisfy the average power constraint $\mathcal{E}\{\|\mathbf{t}_k\|^2\} \leq N$. Note that we impose a power constraint on a per-relay basis rather than a sum power constraint across relay terminals.

As already mentioned above, throughout the paper, path-loss and shadowing is accounted for through the $E_{k,l}$ ($k = 1, 2, \dots, K$; $l = 1, 2, \dots, M$) (for the first hop) and the $P_{l,k}$ ($l = 1, 2, \dots, M$; $k = 1, 2, \dots, K$) (for the second hop). We assume that these parameters, describing the geometry of the network, are deterministic, uniformly bounded from above (follows from the dead-zone assumption) and below (follows from the dense network assumption) so that

$$\underline{E} \leq E_{k,l} \leq \bar{E}, \quad \underline{P} \leq P_{l,k} \leq \bar{P}, \quad \forall k, l. \quad (3)$$

Throughout the paper, we assume that the source terminals \mathcal{S}_l do not have channel state information (CSI). The assumptions on CSI at the relays and the destination terminals will be made specific when discussing P1 and P2 in the next section and when stating our results in Sections 4 and 5.

3 P1 and P2 for Multiple-Antenna Relays

In this section, we briefly formulate (straightforward) modifications of P1 and P2, as summarized in [13], to take into account the presence of multiple-antenna relays, where the individual antenna elements on a given relay are allowed to cooperate. As demonstrated in [13], P1 and P2 trade off the amount of CSI required at the relay terminals for the number of relay terminals needed (asymptotically in M and K) to obtain a given per source-destination terminal pair capacity. We shall see that the same conclusion applies to the multiple-antenna relay versions of P1 and P2. The main focus of this paper is, however, on the impact of cooperation at the relay level and on the network outage behavior.

3.1 P1 for multiple-antenna relays

The basic setup was introduced in Section 2. We shall next describe the specifics of P1 for multiple-antenna relays. A more detailed description (for the multiple-antenna relay case) can be found in [1]. The K relay terminals are partitioned into M subsets \mathcal{M}_l ($l = 1, 2, \dots, M$) with $|\mathcal{M}_l| = K/M$. The relays in \mathcal{M}_l are assumed to assist the l th source-destination terminal pair $\{\mathcal{S}_l, \mathcal{D}_l\}$. For simplicity of notation, we introduce the relay partitioning function $p : [1, K] \rightarrow [1, M]$ defined as

$$p(k) = l \Leftrightarrow \mathcal{R}_k \in \mathcal{M}_l.$$

We assume that the k th relay terminal has perfect knowledge of the phases of the single-input multiple-output backward channel $\mathcal{S}_{p(k)} \rightarrow \mathcal{R}_k$ given by

$$\tilde{\mathbf{h}}_{k,p(k)} = \left[e^{j\arg([\mathbf{h}_{k,p(k)}]_1)} \ e^{j\arg([\mathbf{h}_{k,p(k)}]_2)} \ \dots \ e^{j\arg([\mathbf{h}_{k,p(k)}]_N)} \right]^T \quad (4)$$

and the phases of the corresponding multiple-input single-output forward channel $\mathcal{R}_k \rightarrow \mathcal{D}_{p(k)}$ given by

$$\tilde{\mathbf{f}}_{p(k),k}^T = \left[e^{j\arg([\mathbf{f}_{p(k),k}]_1)} \ e^{j\arg([\mathbf{f}_{p(k),k}]_2)} \ \dots \ e^{j\arg([\mathbf{f}_{p(k),k}]_N)} \right]. \quad (5)$$

Here $[\mathbf{h}_{k,l}]_i$ and $[\mathbf{f}_{l,k}]_i$ denote the i th element of the vector $\mathbf{h}_{k,l}$ and $\mathbf{f}_{l,k}$, respectively. The signal \mathbf{r}_k received at the k th relay terminal is phase-matched-filtered with respect to (w.r.t.) the assigned backward channel followed by a normalization so that

$$u_k = \tau_k^{(1)} \tilde{\mathbf{h}}_{k,p(k)}^H \mathbf{r}_k \quad (6)$$

where $\tau_k^{(1)} = (\sum_{l=1}^M E_{k,l} + \frac{\pi}{4}N(N-1)E_{k,p(k)} + N\sigma^2)^{-1/2}$ ensures $\mathcal{E}\{|u_k|^2\} = 1$. Relay terminal \mathcal{R}_k then computes the transmit signal \mathbf{t}_k by transmit phase-matched-filtering w.r.t. its assigned forward channel, i.e., by computing

$$\mathbf{t}_k = \tilde{\mathbf{f}}_{p(k),k}^* u_k \quad (7)$$

which obviously satisfies the power constraint $\mathcal{E}\{\|\mathbf{t}_k\|^2\} = N$. In summary, P1 ensures that the relays $\mathcal{R}_k \in \mathcal{M}_l$ forward the signal intended for \mathcal{D}_l in a “doubly coherent” (w.r.t. backward and forward channel) fashion whereas the signals transmitted by the source terminals \mathcal{S}_m with $m \neq l$ are forwarded to \mathcal{D}_l in a “noncoherent” fashion (i.e., phase incoherence occurs either on the backward or the forward link or on both links). We conclude by noting that cooperation in groups of N relay antenna elements is achieved by phase combining on the backward and forward links of each relay.

3.2 P2 for multiple-antenna relays

The only difference between P1 and P2 is in the processing at the relays. Whereas in P1 the K relay terminals are partitioned into M clusters (of equal size) with each of these clusters assisting one particular source-destination terminal pair, in P2 each relay assists all source-destination terminal pairs so that relay partitioning is not needed. In turn P2 requires that each relay knows the phases of all its M backward and M forward vector

channels, i.e., \mathcal{R}_k needs knowledge of $\tilde{\mathbf{h}}_{k,l}$ and $\tilde{\mathbf{f}}_{l,k}$, respectively, for $l = 1, 2, \dots, M$. Consequently P2 requires significantly more CSI at the relays than P1. The relay processing stage in P2 computes

$$\mathbf{t}_k = \tau_k^{(2)} \left(\sum_{l=1}^M \tilde{\mathbf{f}}_{l,k}^* \tilde{\mathbf{h}}_{k,l}^H \right) \mathbf{r}_k$$

where $\tau_k^{(2)} = \left(M \sum_{l=1}^M E_{k,l} + \frac{\pi}{4} N(N-1) \sum_{l=1}^M E_{k,l} + MN\sigma^2 \right)^{-1/2}$ ensures that the power constraint $\mathcal{E}\{\|\mathbf{t}_k\|^2\} = N$ is satisfied. Just like in P1, we have cooperation at the relay level in groups of N antenna elements.

4 Capacity Scaling Results

In this section, we provide our results on the ergodic capacity scaling behavior of protocols P1 and P2 described in the previous section. The two main statements are summarized as follows^{4,5}.

Theorem 1 (Ergodic capacity of P1). *Suppose that destination terminal \mathcal{D}_l ($l = 1, 2, \dots, M$) has perfect knowledge of the mean of the effective channel gain of the $\mathcal{S}_l \rightarrow \mathcal{D}_l$ link, given by $(\pi/4)N^2 \sum_{k:p(k)=l} \tau_k^{(1)} \sqrt{E_{k,l} P_{l,k}}$. Then, for any $\epsilon > 0$ there exist M_0, K_0 , such that for all $M \geq M_0, K \geq K_0$, the per source-destination terminal pair capacity achieved by P1 satisfies*

$$\frac{1}{2} \log \left(1 + \frac{\pi^2 \underline{P} \underline{E}^2}{16 \overline{P} \overline{E}^2} \frac{KN^2}{M^3} \right) - \epsilon \leq C_{P1} \leq \frac{1}{2} \log \left(1 + \frac{\pi^2 \overline{P} \overline{E}^2}{16 \underline{P} \underline{E}^2} \frac{KN^2}{M^3} \right) + \epsilon. \quad (8)$$

Theorem 2 (Ergodic capacity of P2). *Suppose that destination terminal \mathcal{D}_l ($l = 1, 2, \dots, M$) has perfect knowledge of the mean of the effective channel gain of the $\mathcal{S}_l \rightarrow \mathcal{D}_l$ link, given by $(\pi/4)N^2 \sum_{k=1}^K \tau_k^{(2)} \sqrt{E_{k,l} P_{l,k}}$. Then, for any $\epsilon > 0$ there exist M_0, K_0 , such that for all $M \geq M_0, K \geq K_0$, the per source-destination terminal pair capacity achieved by P2 satisfies*

$$\frac{1}{2} \log \left(1 + \frac{\pi^2 \underline{P} \underline{E}^2}{16 \overline{P} \overline{E}^2} \frac{KN^2}{M^2} \right) - \epsilon \leq C_{P2} \leq \frac{1}{2} \log \left(1 + \frac{\pi^2 \overline{P} \overline{E}^2}{16 \underline{P} \underline{E}^2} \frac{KN^2}{M^2} \right) + \epsilon. \quad (9)$$

The proofs of Theorems 1 and 2 are lengthy and can be found in [15]. The technique used to prove the lower bounds in (8) and (9) is identical to the technique used in the proof of [13, Theorem 1]. The method used to prove the upper bounds in Theorems 1 and 2 is based on the convergence results for the individual link SINRs reported in Theorems 3 and 4 in the next section.

The results in Theorems 1 and 2 are asymptotic in M and K . For the lower bounds in (8) and (9) we can, however, state a stronger result which is valid in the finite M and K case. In particular, we have

$$C_{P1} \geq \frac{1}{2} \log \left(1 + \frac{A_{P1}}{B_{P1}} \right) \quad (10)$$

⁴The dependence on $N, \underline{E}, \overline{E}, \underline{P}$ and \overline{P} only makes the results in Theorems 1 and 2 uniformly valid over the source-destination pairs $l = 1, 2, \dots, M$.

⁵Strictly speaking, the upper bounds in the form specified in Theorems 1 and 2 hold for $K > M^2$ in P1 and $K > M$ in P2 only. If $K < M^2$ in P1 or $K < M$ in P2, the second term inside the log of the upper bounds in (8) and (9) still goes to zero for $M \rightarrow \infty$, albeit at a different rate which can be shown to be at least $1/M$ [15].

where

$$\begin{aligned}
A_{P1} &= \frac{\pi^2}{16} K^2 N^4 \underline{P} \underline{E} \\
B_{P1} &= \eta \overline{P} \overline{E} \left(\left(1 - \frac{\pi}{4}\right)^2 KM N^2 + \left(1 - \frac{\pi}{4}\right) \frac{\pi}{2} KM N^3 \right) + \\
&+ \eta \overline{P} \overline{E} \left(3KM(M-1)N^2 \frac{\pi}{2} KM(M-1)N^2(N-1) + KM(M-2)(M-1)N^2 \right) \\
&+ \eta \overline{P} \left(\frac{\pi}{4} KM N^2(N-1)\sigma^2 + KM^2 N^2 \sigma^2 \right) \\
&+ \overline{E} M^3 \sigma^2 + \frac{\pi}{4} \overline{E} N(N-1)M^2 \sigma^2 + NM^2 \sigma^4
\end{aligned}$$

with

$$\eta = \frac{M\overline{E} + \frac{\pi}{4}N(N-1)\overline{E} + N\sigma^2}{M\overline{E} + \frac{\pi}{4}N(N-1)\underline{E} + N\sigma^2}.$$

The corresponding result for P2 is given by

$$C_{P2} \geq \frac{1}{2} \log \left(1 + \frac{A_{P2}}{B_{P2}} \right) \quad (11)$$

where $A_{P2} = A_{P1}$ and $B_{P2} = B_{P1}/M$.

Discussion of results. The results in Theorems 1 and 2 can be summarized as⁶

$$C_{P1} = \frac{1}{2} \log \left(1 + \Theta \left(\frac{KN^2}{M^3} \right) \right), \quad C_{P2} = \frac{1}{2} \log \left(1 + \Theta \left(\frac{KN^2}{M^2} \right) \right).$$

Similar to [13], we can conclude that asymptotically in M if $K \propto M^\alpha$ with $\alpha \geq 3$ in P1 and $\alpha \geq 2$ in P2 both protocols achieve distributed orthogonalization, i.e., the effective MIMO channel matrix between the source and destination terminals is diagonalized (in a completely decentralized fashion) resulting in full sum capacity pre-log despite the fact that the destination terminals cannot cooperate. Equivalently, we can say that the network decouples (into isolated source-destination pair links). The per-stream array gain A given by $A_{P1} = KN^2/M^3$ for P1 and $A_{P2} = KN^2/M^2$ for P2, can be decomposed into a contribution due to distributed array gain, A_d , and a contribution due to cooperation at the relay level (realized by phase matching on backward and forward links), A_c , i.e., $A = A_d A_c$ with $A_{d,P1} = KN/M^3$, $A_{d,P2} = KN/M^2$ and $A_{c,P1} = A_{c,P2} = N$. In order to illustrate the impact of cooperation at the relay level, we compare a network with T noncooperating single-antenna relay terminals to a network with a total of $T = KN$ relay antenna elements cooperating in groups of N antennas. In the single-antenna relay case (i.e., no cooperation at the relay level), we have

$$C_{P1}^{(nc)} = \frac{1}{2} \log \left(1 + \Theta \left(\frac{T}{M^3} \right) \right)$$

whereas in the multi-antenna relay case (i.e., cooperation in groups of N relay antennas)

$$C_{P1}^{(c)} = \frac{1}{2} \log \left(1 + \Theta \left(\frac{TN}{M^3} \right) \right).$$

⁶Note that in this section we use the $\Theta(\cdot)$ -notation only to hide the dependence on \underline{E} , \overline{E} , \underline{P} and \overline{P} . Strictly speaking, as N is finite it should also be hidden under the $\Theta(\cdot)$ -notation. However, our goal is to exhibit the impact of cooperation at the relay level on C_{P1} and C_{P2} , which is the reason for making the dependence on N explicit.

Cooperation at the relay level in groups of N relay antenna elements therefore yields an N -fold increase in the effective per-stream SNR due to additional array gain given by $A_c = N$. Equivalently, the total number of antenna elements at the relay level needed to achieve a given per source-destination terminal pair capacity is reduced by a factor of N through cooperation. The conclusions for P2 are identical.

5 Outage Analysis

The focus in the previous section was on the ergodic capacity scaling behavior of P1 and P2. In this section, we provide results that have an outage analysis flavor.

We start with the following observation. Since the destination terminals \mathcal{D}_l cannot cooperate independent (single-user) decoding has to be performed. The network can therefore be viewed as a collection of M single-input single-output (SISO) channels $\mathcal{S}_l \rightarrow \mathcal{D}_l$ ($l = 1, 2, \dots, M$). Each of these SISO channels will have a random-valued channel gain⁷ g_l (due to the fading nature of the network), a random-valued interference term i_l , caused by the source signals not intended for a given destination terminal, and a (random-valued) noise term n_l consisting of thermal noise forwarded by the relays and thermal noise at the destination terminals. The general form of the input-output relationship for the $\mathcal{S}_l \rightarrow \mathcal{D}_l$ link is therefore given by $y_l = g_l s_l + i_l + n_l$ ($l = 1, 2, \dots, M$). We note that the randomness in i_l comes from the fading coefficients and from interfering signals transmitted by other (than \mathcal{S}_l) source terminals. The randomness in n_l is due to Gaussian noise and fading coefficients. In general neither i_l nor n_l will be Gaussian, which makes the capacity analysis difficult. In this and the next section, we make the conceptual assumption that the destination terminals know the fading coefficients in the entire network, i.e., $\mathbf{h}_{k,l}$ and $\mathbf{f}_{l,k}$ for $l = 1, 2, \dots, M$, $k = 1, 2, \dots, K$, which together with perfect knowledge of⁸ $E_{k,l}$ and $P_{l,k} \forall l, k$ also implies perfect knowledge of g_l at \mathcal{D}_l . We emphasize, however, that the capacity scaling results in Theorems 1 and 2 require only minimal channel knowledge at the destination terminals. Conditioned on $\{\mathbf{h}_{k,l}, \mathbf{f}_{l,k}\}_{\forall l,k}$ both i_l and n_l become Gaussian so that the mutual information for the $\mathcal{S}_l \rightarrow \mathcal{D}_l$ link is given by

$$I_l = \frac{1}{2} \log \left(1 + \text{SINR}_l |_{\{\mathbf{h}_{k,l}, \mathbf{f}_{l,k}\}} \right) \quad \text{with} \quad \text{SINR}_l |_{\{\mathbf{h}_{k,l}, \mathbf{f}_{l,k}\}} = \frac{|g_l|^2}{\sigma_i^2 + \sigma_n^2}$$

where $\sigma_i^2 = \text{VAR}(i_l)$. In the following, we analyze the behavior of the RVs $\text{SINR}_l |_{\{\mathbf{h}_{k,l}, \mathbf{f}_{l,k}\}}$ for P1 and P2 as $M, K \rightarrow \infty$. Since the results in Theorems 3 and 4 are uniformly valid over all source-destination terminal pairs $l = 1, 2, \dots, M$, in the following we shall simply write SINR_{P1} and SINR_{P2} where conditioning on $\{\mathbf{h}_{k,l}, \mathbf{f}_{l,k}\}$ is not made explicit for brevity. Our results show that both SINR_{P1} and SINR_{P2} lie within narrow intervals around their means with high probability when $M, K \rightarrow \infty$. The precise statements are as follows.

Theorem 3. *There exist constants $C_1, C_2, C_3, C_4, C_5, C_6, M_0$ and K_0 (depending on $N, \underline{E}, \bar{E}, \underline{P}$ and \bar{P} only) such that for any $M \geq M_0$ and $K \geq K_0$ for any $x > 1$, the probability*

⁷The following discussion applies to both protocols. For the sake of simplicity of notation we therefore omit the subscripts P1 and P2.

⁸In the following, we shall tacitly assume that $E_{k,l}$ and $P_{l,k} \forall l, k$ is perfectly known at the destination terminals.

$P_{\text{out,P1}}$ of the event $\text{SINR}_{\text{P1}} \notin [L_{\text{P1}}, U_{\text{P1}}]$, where

$$L_{\text{P1}} = \frac{\pi^2 \underline{P} \underline{E}^2}{16 \overline{P} \overline{E}^2} \frac{\left(\max \left[0, N^2 K - C_1 M \sqrt{K} x \right] \right)^2}{N^2 M^2 (M-1) K + C_2 M^{5/2} K x + C_3 M^3} \quad (12)$$

$$U_{\text{P1}} = \frac{\pi^2 \overline{P} \overline{E}^2}{16 \underline{P} \underline{E}^2} \frac{\left(N^2 K + C_4 M \sqrt{K} x \right)^2}{\max[0, N^2 M^2 (M-1) K - C_5 M^{5/2} K x] + C_6 M^3} \quad (13)$$

satisfies the following inequality

$$P_{\text{out,P1}} \leq S_1(M, K) e^{-\Delta_1 x^{2/7}} \quad (14)$$

where $S_1(M, K)$ is a (Laurent) polynomial in M and K depending on $N, \underline{E}, \overline{E}, \underline{P}$ and \overline{P} only and Δ_1 is a constant depending on $N, \underline{E}, \overline{E}, \underline{P}$ and \overline{P} only.

The corresponding result for P2 is given by

Theorem 4. *There exist constants $C_1, C_2, C_3, C_4, C_5, C_6, M_0$ and K_0 (depending on $N, \underline{E}, \overline{E}, \underline{P}$ and \overline{P} only) such that for any $M \geq M_0$ and $K \geq K_0$ for any $x > 1$, the probability $P_{\text{out,P2}}$ of the event $\text{SINR}_{\text{P2}} \notin [L_{\text{P2}}, U_{\text{P2}}]$, where*

$$L_{\text{P2}} = \frac{\pi^2 \underline{P} \underline{E}^2}{16 \overline{P} \overline{E}^2} \frac{\left(\max \left[0, N^2 K - C_1 \sqrt{M} K x \right] \right)^2}{N^2 M (M-1) K + C_2 M^{3/2} K x + C_3 M^2} \quad (15)$$

$$U_{\text{P2}} = \frac{\pi^2 \overline{P} \overline{E}^2}{16 \underline{P} \underline{E}^2} \frac{\left(N^2 K + C_4 \sqrt{M} K x \right)^2}{\max[0, N^2 M (M-1) K - C_5 M^{3/2} K x] + C_6 M^2} \quad (16)$$

satisfies the following inequality

$$P_{\text{out,P2}} \leq S_2(M, K) e^{-\Delta_2 x^{2/7}} \quad (17)$$

where $S_2(M, K)$ is a polynomial in M and K depending on $N, \underline{E}, \overline{E}, \underline{P}$ and \overline{P} only and Δ_2 is a constant depending on $N, \underline{E}, \overline{E}, \underline{P}$ and \overline{P} only.

The proofs of (refined versions) of Theorems 3 and 4 along with exact expressions for $S_1(M, K), S_2(M, K), \Delta_1$ and Δ_2 can be found in [15]. Eqs. (14) and (17) state that the SINRs of the effective channels $\mathcal{S}_l \rightarrow \mathcal{D}_l$ ($l = 1, 2, \dots, M$) for both protocols converge to a deterministic limit as $M, K \rightarrow \infty$. Moreover, it is shown in [15] that the per-stream diversity order approaches ∞ as $M, K \rightarrow \infty$ and hence each of the individual SISO links in the network converges to an AWGN link. In combination with the fact that the network also decouples (cf. Theorems 1 and 2) we say that the fading interference relay network ‘‘crystallizes’’ to a set of independent AWGN channels.

The results in Theorems 3 and 4 have the flavor of an outage analysis in the sense of characterizing the rate of convergence (for $M, K \rightarrow \infty$) of the individual SISO fading links to AWGN links. Indeed, as shown in [15], Theorems 3 and 4 can be reformulated to provide bounds on the outage probability. For small M and K , the bounds in (14) and (17), however, tend to be loose. We finally note that the exponent $2/7$ in (14) and (17) is unlikely to be fundamental and is probably a consequence of our proof technique. In this sense Theorems 3 and 4 should be understood as quantifying a guaranteed rate of convergence rather than the best possible.

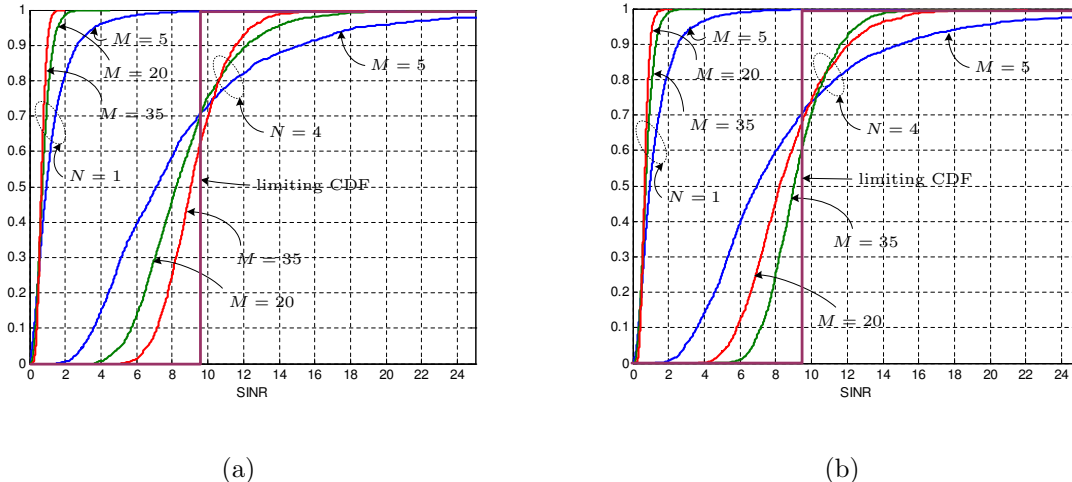


Figure 2: Simulated (Monte-Carlo) SINR CDFs for different values of M , $N = 1$ and $N = 4$ for (a) $K = M^3$ in P1 and (b) $K = M^2$ in P2.

6 Numerical Results

The goal of this section is to numerically characterize the convergence behavior (as $M, K \rightarrow \infty$) of the individual fading SISO links $\mathcal{S}_l \rightarrow \mathcal{D}_l$ to AWGN links.

In all simulation results below, we set $E_{k,l} = P_{l,k} = 1 \forall l, k$ and $\sigma^2 = 0.01$. This choice for the path loss and shadowing parameters, although not representative of a real-world scenario, isolates the dependence of our results on the network geometry. Moreover, the distribution of the different SINR RVs for a given protocol is identical for all links so that it suffices to analyze the behavior of only one SINR RV for each of the two protocols.

For $K = M^3$ in P1 and $K = M^2$ in P2, Fig. 2 shows the cumulative distribution functions (CDFs) (obtained through Monte-Carlo methods) of SINR_{P1} and SINR_{P2} , respectively, for different values of M and N . We observe that for increasing M , with N fixed, the CDFs approach a step function at the corresponding mean values, i.e., the SINR RVs converge to a deterministic quantity and consequently the underlying fading channel converges to an AWGN channel. We can furthermore see that for fixed M and fixed N the CDFs are very similar for P1 and P2 suggesting that the convergence behavior is similar for the two protocols. Recall, however, that $K = M^3$ in P1 and $K = M^2$ in P2. Finally, we note that increasing N for fixed M results in higher per source-destination terminal pair capacity (cf. Theorems 1 and 2) but at the same time “slows down convergence” (w.r.t. M and hence also K) to the deterministic limit.

7 Conclusion

For a fading interference relay network, we showed that cooperation at the relay level results in a reduction of the total number of relay terminal antennas needed to achieve a given per source-destination terminal pair capacity. Furthermore, we characterized the convergence behavior of the individual fading source-destination terminal pair links to AWGN links thereby establishing a guaranteed rate at which the network “crystallizes” when the number of nodes gets large.

References

- [1] H. Bölcskei, R. U. Nabar, Ö. Oyman, and A. J. Paulraj, “Capacity scaling laws in MIMO relay networks,” *IEEE Trans. Wireless Commun.*, 2006, to appear.
- [2] A. F. Dana and B. Hassibi, “On the power efficiency of sensory and ad-hoc wireless networks,” *IEEE Trans. Inf. Theory*, 2003, submitted.
- [3] P. Gupta and P. R. Kumar, “The capacity of wireless networks,” *IEEE Trans. Inf. Theory*, vol. 46, no. 2, pp. 388–404, March 2002.
- [4] M. Gastpar and M. Vetterli, “On the capacity of wireless networks: The relay case,” in *Proc. IEEE INFOCOM*, vol. 3, New York, NY, June 2002, pp. 1577–1586.
- [5] M. Grossglauser and D. Tse, “Mobility increases the capacity of ad hoc wireless networks,” *IEEE/ACM Trans. Networking*, vol. 10, no. 4, pp. 477–486, Aug. 2002.
- [6] O. Lévêque and I. E. Telatar, “Information-theoretic upper bounds on the capacity of large extended ad hoc wireless networks,” *IEEE Trans. Inf. Theory*, vol. 51, no. 3, pp. 858–865, March 2005.
- [7] L. Xie and P. R. Kumar, “A network information theory for wireless communication: Scaling laws and optimal operation,” *IEEE Trans. Inf. Theory*, vol. 50, no. 5, pp. 748–767, May 2004.
- [8] J. N. Laneman and G. W. Wornell, “Distributed space-time-coded protocols for exploiting cooperative diversity in wireless networks,” *IEEE Trans. Inf. Theory*, vol. 49, no. 10, pp. 2415–2425, Oct. 2003.
- [9] G. Kramer, M. Gastpar, and P. Gupta, “Cooperative strategies and capacity theorems for relay networks,” *IEEE Trans. Inf. Theory*, vol. 51, no. 9, pp. 3037–3063, Sept. 2005.
- [10] B. Wang, J. Zhang, and A. Høst-Madsen, “On the capacity of MIMO relay channels,” *IEEE Trans. Inf. Theory*, vol. 51, no. 1, pp. 29–43, Jan. 2005.
- [11] R. U. Nabar, H. Bölcskei, and F. W. Kneubühler, “Fading relay channels: Performance limits and space-time signal design,” *IEEE J. Sel. Areas Commun.*, vol. 22, no. 6, pp. 1099–1109, Aug. 2004.
- [12] A. Jovičić, P. Viswanath, and S. R. Kulkarni, “Upper bounds to transport capacity of wireless networks,” *IEEE Trans. Inf. Theory*, vol. 50, no. 11, pp. 2555–2565, Nov. 2004.
- [13] V. I. Morgenshtern, H. Bölcskei, and R. U. Nabar, “Distributed orthogonalization in large interference relay networks,” in *Proc. IEEE ISIT*, Adelaide, Australia, Sept. 2005, pp. 1211–1215.
- [14] M. Médard, “The effect upon channel capacity in wireless communications of perfect and imperfect knowledge of the channel,” *IEEE Trans. Inf. Theory*, vol. 46, no. 3, pp. 933–946, May 2000.
- [15] V. I. Morgenshtern and H. Bölcskei, “Crystallization in large interference relay networks,” in preparation.